Optics Letters

Synthesis of the Einstein–Podolsky–Rosen entanglement in a sequence of two single-mode squeezers

Ilya A. Fedorov,[1,2] Alexander E. Ulanov,[1,3] Yury V. Kurochkin,[1] and A. I. Lvovsky[1,2,4,*]

[1]Russian Quantum Center, 100 Novaya St., Skolkovo, Moscow 143025, Russia
[2]P. N. Lebedev Physics Institute, Leninskiy Prospect 53, Moscow 119991, Russia
[3]Moscow Institute of Physics and Technology, 141700 Dolgoprudny, Russia
[4]Institute for Quantum Science and Technology, University of Calgary, Calgary AB T2N 1N4, Canada
*Corresponding author: LVOV@ucalgary.ca

Received 2 November 2016; revised 30 November 2016; accepted 1 December 2016; posted 6 December 2016 (Doc. ID 280015); published 23 December 2016

We propose and implement a new scheme of generating the optical Einstein–Podolsky–Rosen entangled state. Parametric down-conversion in two nonlinear crystals, positioned back-to-back in the waist of a pump beam, produces single-mode squeezed vacuum states in orthogonal polarization modes; a subsequent beam splitting entangles them and generates the Einstein–Podolsky–Rosen state. The technique takes advantage of the strong nonlinearity associated with type-0 phase-matching configuration while, at the same time, eliminating the need for actively stabilizing the optical phase between the two single-mode squeezers. We demonstrate our method, preparing a 1.4 dB two-mode squeezed state and characterizing it via two-mode homodyne tomography.

OCIS codes: (190.4970) Parametric oscillators and amplifiers; (270.6570) Squeezed states; (270.5585) Quantum information and processing.

https://doi.org/10.1364/OL.42.000132

The two-mode squeezed vacuum state is characterized by simultaneous correlation of the positions and anticorrelation of the momenta of two harmonic oscillators beyond the standard quantum limit defined by the vacuum state. Discovered in 1935 by Einstein, Podolsky, and Rosen [1], this state (which we hereafter refer to as the EPR state) gave rise to the celebrated quantum nonlocality paradox. With the emergence of quantum-optical information technology, the EPR state became the primary entangled resource for the continuous variable domain. Its applications include quantum information processing [2,3], quantum metrology [4–8], quantum imaging [8,9] quantum cryptography [10,11], teleportation [12], and quantum repeater [13,14] protocols.

While the EPR state can be prepared in a variety of nonlinear physical media, such as atomic ensembles [9] and fibers [15], the most common approach employs spontaneous parametric down-conversion (SPDC) in a crystal with second-order nonlinearity. If SPDC is utilized in the nondegenerate configuration, the EPR state is produced directly in its two output channels [16,17]. This approach, however, is associated with certain challenges. In particular, if the SPDC is noncollinear, critical phase matching may complicate the optical alignment or distort the emission modes. Furthermore, such an arrangement is difficult to set up within a Fabry–Perot resonator. In collinear SPDC settings, on the other hand, the emission modes are typically separated by means of the type-2 phase-matching configuration in which the signal and idler fields are orthogonally polarized. In many crystals, however, such an arrangement has significantly lower nonlinear coefficients than type-0, in which the pump, signal, and idler fields have the same polarization [18].

Therefore, a frequently employed alternative approach is to first obtain single-mode position- and momentum-squeezed states in two independent optical modes via degenerate SPDC and, subsequently, make them interfere on a symmetric beam splitter [12,19,20]. The quadrature operators of the two modes then transform according to

$$\begin{bmatrix} X_1' \\ X_2' \end{bmatrix} = \frac{1}{\sqrt{2}} \begin{bmatrix} 1 & -1 \\ 1 & 1 \end{bmatrix} \begin{bmatrix} X_1 \\ X_2 \end{bmatrix}, \tag{1}$$

producing the two-mode squeezed state at the output. While this method allows one to obtain high degrees of squeezing [20], it requires precise phase locking between the two squeezed light sources, which is a significant technical complication.

In this Letter, we propose a scheme devoid of these drawbacks. The idea, inspired by Kwiat *et al.* [21], is to use a series of two degenerate SPDC processes, placing the two nonlinear crystals in a single waist of the pump beam immediately one after another (Fig. 1). If the optical axes of the crystals are orthogonal to each other, and the pump beam is polarized diagonally between them, the two nonlinear processes will squeeze orthogonally polarized vacuum modes. The two squeezed vacua thereby populate a single spatial mode and

can be put to interference using a pair of wave plates. Since the distance between the crystals is limited by a few millimeters, air density fluctuations between the two squeezed vacua are negligible, so no phase locking is required.

Concurrent interaction in second-order nonlinear media of multiple configurations has also been used in the continuous variable domain, albeit in configurations different from ours. In particular, the Pfister group has demonstrated concurrent second-harmonic generation from all three possible nonlinearities in $KTiPO_4$ using a nonlinear crystal with a complex periodic poling structure [22,23]. Subsequently, they used such a crystal to prepare quadripartite cluster entanglement in the optical frequency comb [24]. In 2014, a more complex cluster entanglement has been achieved with two periodically poled crystals placed in two waists of an optical parametric amplifier cavity [25].

In our experiment, both down-conversion processes take place in periodically poled potassium titanyl-phosphate crystals. The first and second crystals are phase matched for type-0 degenerate SPDC into the vertical and horizontal polarization modes, respectively. The phase matching is aligned by the independent angle and temperature control of each crystal. The crystals are pumped in a single-pass manner with frequency-doubled pulses at $\lambda = 390$ nm, generated by a Ti:sapphire laser with a repetition rate of 76 MHz and a pulse width of 1.5 ps [26]. The average power of the pump field is 80 mW. The polarization of the pump field is diagonal, so the pump intensity is distributed equally to both nonlinear processes. After the crystals, the pump field is eliminated by an interference filter.

The length of the crystals along the beam is 1 mm, as shown in Fig. 1. Both crystals are set in the waist of the focused pump beam with the Gaussian radius of $w_0 = 12.4$ μm, with a corresponding Rayleigh range being $z_R = \pi w_0^2/\lambda = 1.25$ mm. The distance between the crystals is 0.45 mm, so that their centers are 0.72 mm away from the beam waist; the beam width at the center points is then $1.15w_0$.

After the second crystal, two orthogonally polarized squeezed vacua, sharing the same spatial mode, are prepared. To characterize these states, the modes are separated by a polarizing beam splitter (Fig. 1) and subjected to homodyne measurement [27]. The variance of the quadrature data from both squeezed states as a function of phase and time is shown in Fig. 2(a). The sinusoidal behavior of the variance is due to linear variation of the optical phase θ of the local oscillator [28]. This behavior is modeled by a perfect squeezer with a squeezing parameter ζ followed by a loss channel with transmissivity η, in which the quadrature variance is given by [29]

$$\langle X_\theta^2 \rangle = \frac{\eta}{2}(\cosh 2\zeta - \cos 2\theta \sinh 2\zeta) + \frac{1-\eta}{2}. \quad (2)$$

The single-mode experimental data can be fit with this equation using $\zeta = 0.44$, $\eta = 0.52$ [Fig. 2(a)]. The latter figure arises from the cumulative effect of the 85% quantum efficiency of the homodyne detector [27] (including the effect of electronic noise [30]), imperfect mode matching between the signal and the local oscillator (90%) and linear losses, partially associated with gray tracking (85%). An additional effective loss arises from the undesired spatial and spectral correlation of the photon pairs produced in pulsed SPDC [31].

The single-mode squeezed states generated in the two crystals are delayed with respect to one another due to the difference in group velocities of the pump and the signal. The experimentally observed delay of 0.58 mm is in agreement with the prediction based on the Sellmeyer model [32]:

$$v_\lambda = 0.41c, \qquad v_{2\lambda} = 0.52c, \quad (3)$$

with c being the speed of light in vacuum. To compensate for that difference, we retard the vertical polarization component of the pump with respect to the horizontal one, using a birefringent calcite crystal of a length of 3.6 mm. The birefringence of calcite depends on its orientation. We rotate the crystal around the vertical axis, as shown in Fig. 2(a), to optimize the delay between the polarization components of the pump and to set the phase between the two squeezed vacua to $\pi/2$.

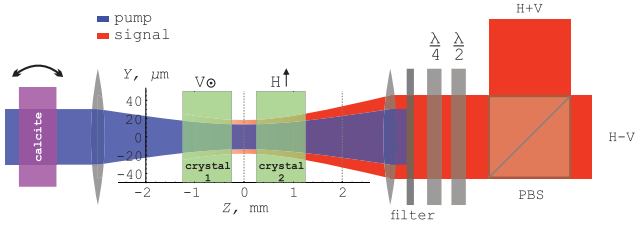

Fig. 1. Schematic of the setup. Both crystals are aligned for collinear, type-0 phase-matching conditions. PBS, polarizing beam splitter. The axes illustrate the longitudinal beam waist behavior and the positioning of the crystals with respect to the waist. Other elements are not drawn to scale.

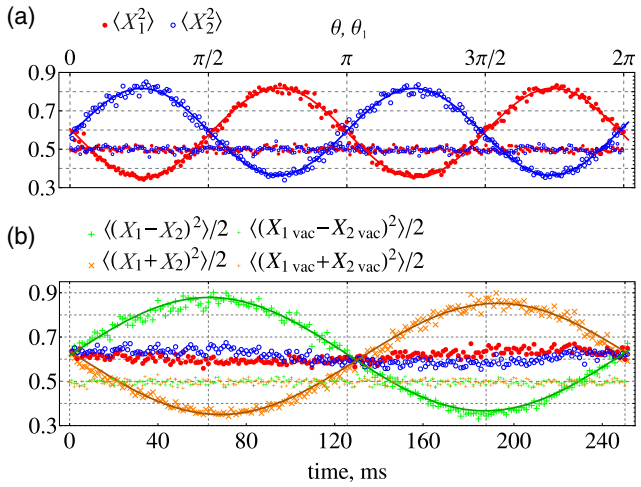

Fig. 2. (a) Variances of the initial, orthogonally squeezed single-mode vacua as a function of time for a linearly varying quadrature phase θ before the interference. Horizontally (vertically) polarized modes: open (filled) circles. The smaller size symbols in the plots correspond to the vacuum state. The lines show the theoretical prediction (2) with $\zeta = 0.44$, detected with an efficiency of 52%. Data are normalized so that the vacuum noise level is 0.5. (b) Variances of the EPR-state quadratures as a function of time. In this experiment, the phase of one of the LOs is varied, θ_1 in (4). Circles, individual quadratures; diagonal/vertical crosses, sum and difference quadratures. The lines show the theoretical prediction for the EPR state (4) with $\zeta = 0.44$ detected with a 50% efficiency. The minimum difference-quadrature variance is 0.36, which corresponds to 1.4 dB of two-mode squeezing.

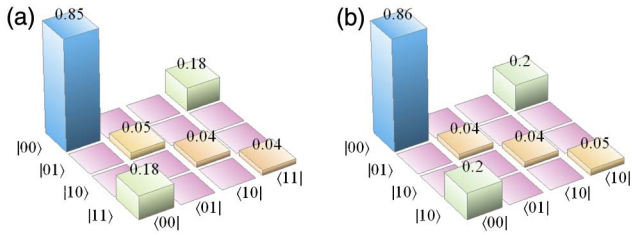

Fig. 3. Reconstructed EPR state (left) and theoretical expectation, based on the experimental input single-mode squeezed states (right). (a) Density matrices in the Fock basis. (b) Correlated probability densities for the position quadratures. The fidelity between the two states is 98%.

The two squeezed states are subsequently brought to interference. The latter is realized in the polarization basis by means of a half-wave plate with its optical axis at 22.5° to horizontal, and a quarter-wave plate for fine tuning. The interfered modes are spatially separated on the polarizing beam splitter and directed to homodyne detectors [27].

The quadrature variances from each individual mode are shown in Fig. 2(b) in blue and purple. Both exhibit approximately constant variance as expected for the EPR state, whose individual modes considered separately are in a thermal state [29]. The sum- and difference- quadrature variances, shown in green and orange, demonstrate opposite phase-dependent variance characteristics of the EPR state. The theoretical expectation for these variances is [13]

$$\left\langle \frac{[X_{1,\theta_1} \mp X_{2,\theta_2}]^2}{2} \right\rangle = \frac{\eta}{2}[\cosh(2\zeta) \pm \cos(\theta_1 + \theta_2)\sinh(2\zeta)] + \frac{1-\eta}{2} \quad (4)$$

and the best fit is obtained with $\zeta = 0.44, \eta = 0.50$. The small decrease in the efficiency with respect to the single-mode case is attributed to the non-ideal interference of the input states, which also explains the residual phase dependence of the individual quadrature variances, visible in Fig. 2(b). Note that, compared to the single-mode squeezed vacua [Fig. 2(a)], the two-mode quadrature variances oscillate at half-frequency, as expected from Eqs. (2) and (4).

The result of two-mode homodyne tomography of the EPR state [33] is presented in Fig. 3, left. The mean photon population of each mode is 0.11, which is in agreement with the expected value $\eta\zeta^2 = 0.10$. The right side of Fig. 3 shows the theoretical expectation [29] with the squeezing and efficiency correction for $\eta = 0.5$. Its fidelity with the experimentally reconstructed state is 98%, the discrepancies being on the order of state reconstruction uncertainties [28].

In summary, we have demonstrated the preparation of the two-mode squeezed vacuum state in a series of two type-0 nonlinear crystals positioned back-to-back in a waist of the pump beam. The demonstrated technique can be seen as continuous variable analog of the method for generating polarization-entangled photon pairs [21]. It takes advantage of the relative strength of optical nonlinearity in type-0 SPDC while eliminating the need for critical phase matching and the phase locking of two independent squeezers. It can be adapted to cavity- or fiber-based optical parametric amplifier schemes.

Funding. Ministry of Education and Science of the Russian Federation (Minobrnauka) (Agreement 14.582.21.0009, ID RFMEFI58215X0009).

Acknowledgment. The authors also thank O. Pfister for helpful discussions.

REFERENCES

1. A. Einstein, B. Podolsky, and N. Rosen, Phys. Rev. **47**, 777 (1935).
2. S. L. Braunstein and P. van Loock, Rev. Mod. Phys. **77**, 513 (2005).
3. U. L. Andersen, G. Leuchs, and C. Silberhorn, Laser Photon. Rev. **4**, 337 (2010).
4. V. Giovannetti, S. Lloyd, and L. Maccone, Science **306**, 1330 (2004).
5. P. M. Anisimov, G. M. Raterman, A. Chiruvelli, W. N. Plick, S. D. Huver, H. Lee, and J. P. Dowling, Phys. Rev. Lett. **104**, 103602 (2010).
6. S. Steinlechner, J. Bauchrowitz, M. Meinders, H. Müller-Ebhardt, K. Danzmann, and R. Schnabel, Nat. Photonics **7**, 626 (2013).
7. R. C. Pooser and B. Lawrie, Optica **2**, 393 (2015).
8. J. B. Clark, Z. Zhou, Q. Glorieux, A. M. Marino, and P. D. Lett, Opt. Express **20**, 17050 (2012).
9. V. Boyer, A. Marino, R. Pooser, and P. Lett, Science **321**, 544 (2008).
10. T. C. Ralph, Phys. Rev. A **61**, 010303 (1999).
11. L. S. Madsen, V. C. Usenko, M. Lassen, R. Filip, and U. L. Andersen, Nat. Commun. **3**, 1083 (2012).
12. A. Furusawa, J. L. Sorensen, S. L. Braunstein, C. A. Fuchs, H. J. Kimble, and E. S. Polzik, Science **282**, 706 (1998).
13. Y. Kurochkin, A. S. Prasad, and A. I. Lvovsky, Phys. Rev. Lett. **112**, 070402 (2014).
14. A. E. Ulanov, I. A. Fedorov, A. A. Pushkina, Y. Kurochkin, T. C. Ralph, and A. I. Lvovsky, Nat. Photonics **9**, 764 (2015).
15. C. Silberhorn, P. K. Lam, O. Weiß, F. König, N. Korolkova, and G. Leuchs, Phys. Rev. Lett. **86**, 4267 (2001).
16. Z. Y. Ou, S. F. Pereira, H. J. Kimble, and K. C. Peng, Phys. Rev. Lett. **68**, 3663 (1992).
17. Y. Zhou, X. Jia, F. Li, C. Xie, and K. Peng, Opt. Express **23**, 4952 (2015).
18. V. G. Dmitriev, G. G. Gurzadyan, and D. N. Nikogosyan, *Handbook of Nonlinear Optical Crystals*, 1st ed. (1993).
19. S. Takeda, T. Mizuta, M. Fuwa, P. van Loock, and A. Furusawa, Nature **500**, 315 (2013).
20. T. Eberle, V. Händchen, and R. Schnabel, Opt. Express **21**, 11546 (2013).
21. P. G. Kwiat, E. Waks, A. G. White, I. Appelbaum, and P. H. Eberhard, Phys. Rev. A **60**, R773 (1999).
22. R. C. Pooser and O. Pfister, Opt. Lett. **30**, 2635 (2005).
23. M. Pysher, A. Bahabad, P. Peng, A. Arie, and O. Pfister, Opt. Lett. **35**, 565 (2010).
24. M. Pysher, Y. Miwa, R. Shahrokhshahi, R. Bloomer, and O. Pfister, Phys. Rev. Lett. **107**, 030505 (2011).
25. M. Chen, N. C. Menicucci, and O. Pfister, Phys. Rev. Lett. **112**, 120505 (2014).
26. S. R. Huisman, N. Jain, S. A. Babichev, F. Vewinger, A.-N. Zhang, S.-H. Youn, and A. I. Lvovsky, Opt. Lett. **34**, 2739 (2009).
27. R. Kumar, E. Barrios, A. MacRae, E. Cairns, E. H. Huntington, and A. I. Lvovsky, Opt. Commun. **285**, 5259 (2012).
28. A. I. Lvovsky and M. G. Raymer, Rev. Mod. Phys. **81**, 299 (2009).
29. A. I. Lvovsky, *Photonics Volume 1: Fundamentals of Photonics and Physics*, D. Andrews, ed. (Wiley, 2015).
30. J. Appel, D. Hoffman, E. Figueroa, and A. I. Lvovsky, Phys. Rev. A **75**, 035802 (2007).
31. A. I. Lvovsky, W. Wasilewski, and K. Banaszek, J. Mod. Opt. **54**, 721 (2007).
32. J. D. Bierlein and H. Vanherzeele, J. Opt. Soc. Am. B **6**, 622 (1989).
33. J. Řeháček, Z. Hradil, E. Knill, and A. I. Lvovsky, Phys. Rev. A **75**, 042108 (2007).